Peculiar self-nucleation behavior of a polybutene-1/ethylene random copolymer

Zefan Wang[1,2], Xia Dong[1,2], Dario Cavallo*, Dujin Wang and Alejandro J. Müller*

Dr. Zefan Wang[1,2], Prof. Xia Dong[1,2], Prof. Dujin Wang[1,2]

[1]Beijing National laboratory for Molecular Science, CAS Key Laboratory of Engineering Plastics, Institute of Chemistry, Chinese Academy of Sciences, Beijing 100190, China

[2]University of Chinese Academy of Sciences, Beijing 100049, China

Prof. Dario Cavallo[3]
[3]Department of Chemistry and Industrial Chemistry, University of Genova, via Dodecaneso, 31 - 16146 Genova, Italy
Email: dario.cavallo@unige.it

Prof. Alejandro J. Müller[4,5]
[4]POLYMAT and Department of Polymers and Advanced Materials: Physics, Chemistry and Technology, Faculty of Chemistry, University of the Basque Country UPV/EHU, Paseo Manuel de Lardizabal 3, Donostia-San Sebastián, 20018, Spain
Email: alejandrojesus.muller@ehu.es

[5]Ikerbasque, Basque Foundation for Science, Bilbao, 48009, Spain

Keywords: polybutene-1, self-nucleation, melt memory

Abstract

The self-nucleation behavior of a polybutene-1/ethylene random copolymer, P(B1-*ran*-E), which undergoes a complex crystal-crystal transition behavior, has been studied in detail. Similar to PE random copolymers, this material shows a strong melt memory effect even above equilibrium melting point of PB-1 homopolymer. Different polymorphic forms can be obtained when P(B1-*ran*-E) is cooled from different self-nucleation *Domains*. The trigonal form I' could only be nucleated in the presence of remaining form I crystals via self-seeding, while the melt memory in *Domain IIa* could only act as self-nuclei for kinetically favored form II. Furthermore, observations from optical microscopy illustrated that melt memory is able to enhance nucleation density but it does not affect the spherulitic growth rate.

1. Introduction

As a basic topic for polymer crystallization, self-nucleation (SN) and the melt memory effect have been investigated for many years. [1-7] Six decades ago, the SN method was employed by Keller et al. [8,9] who produced the first self-nucleated polyethylene single crystals from solution. Vidotto et al. [10] proposed that the number of surviving nuclei after melting depends on temperature and holding time in the melt state. The first attempt of exploring the SN behavior of polymers by differential scanning calorimetry (DSC) was made by Lotz et al. [7,11-14] According to their definition, three classic self-nucleation temperature (T_s) domains were proposed: isotropic melt (*Domain I*), self-nucleation (*Domain II*) as well as self-nucleation and annealing (*Domain III*) domains.

Due to the constraining effects of entanglements, long chain polymers usually need long time to relax after melting. Some ordered structure preserved from the previous crystalline state could serve as an efficient nucleator in the following crystallization process. [7] This phenomenon is called "melt memory effect". However, there is still a debate on the properties of the remaining self-nuclei, because no characterization method can detect specific signals after melting. [6,15,16] A recent review on melt memory has been published by Sangroniz et al. [17]

Strobl et al. [18-20] considered that melt memory is a mesomorphic phase, which can be in-filled with crystals upon cooling. According to their observations, both nucleation density and growth rate of polymer crystals can be promoted by the presence of this mesomorphic phase that could be considered as a kind of self-nuclei. Based on

simulation results, Luo and Sommer[21-24] claimed that the melt memory inherited from crystals is an entangled state with lower entanglement density after melting, which can serve as active nucleation sites.

Müller et al. [7,17,25] proposed that the melt memory effect is due to remaining segmental orientation of the chains originally packed in the crystals. By employing different families of polymers with interacting functional groups (amides, esters, carbonates and ethers), it has been recently demonstrated that intermolecular interactions allow chains to retain their segmental orientation in self-nucleated melts. [17,25-27] Müller et al. also explored how temperature and time affect melt memory and have shown that it is a largely kinetic effect. [7,17,25,28] Furthermore, recently, they have proposed to divide the self-nucleation domain or *Domain II* into 2 sub-domains. *Domain IIa* (or melt memory sub-domain) occurs at self-nucleation temperatures above the end temperature of melting of all crystals in the sample, as determined by DSC. *Domain IIb* on the other hand is a self-seeding sub-domain, where most of the polymer crystals are melted, but small crystal fragments remain.[7,17]

Alamo et al. [15,16,29] observed an unexpected strong melt memory effect in polyethylene copolymers above the equilibrium melting temperature. They interpreted the mechanism behind this peculiar phenomenon as the formation of a complex topology of knots, loops, ties, and other entanglements within the inter-crystalline regions, which are caused by the selection and dragging process of polymer chains when suitable ethylene sequences with low branch contents are packed into the lattice. On the other hand, memory effects can also be produced by shear flow in polymer melts

due to chain orientation. [30-34] Hsiao et al. [30,31] proposed that shear-induced precursors with some content of long helices do not have crystallographic structure and can survive at relatively high temperatures.

Due to the complicated solid-solid transition of polybutene-1 (PB-1) homopolymer and its copolymer, self-nucleation behavior of this material has attracted much interest. Detailed crystal structure and formation route of PB-1 homopolymer polymorphs are summarized in Table S1. The self-nucleation behavior of ~~polybutene-1 homopolymer~~ form I crystals has been carefully investigated by Cavallo et al. [33,35-38] With specifically designed thermal treatments, the authors found that only the kinetically favored form II could be nucleated onto the surface of form I spherulites, a phenomenon denoted "cross-nucleation".[37] However, via DSC and synchrotron IR microspectroscopy, small amount of form I' crystals with similar crystal structure was observed to be generated within the interior of the spherulite by self-seeding. [35,36,38] In addition, the melt memory domain of PB-1 is relatively narrow like polyethylene, polypropylene and other non-polar homopolymers. [26,39] In our recent work,[40] a very small fraction of trigonal form I crystals was observed transforming from form II after annealing at 0 °C for very short time. Comparing to PB-1, a large amount of form I' crystals in the copolymer P(B1-*ran*-E) could be formed in the presence of a small amount of form I crystals.

With the interest of understanding the complex solid-solid transitions in PB-1 based polymers, the self-nucleation behavior of a PB-1/ethylene random copolymer, P(B1-*ran*-E), has been investigated in detail in this study. Similar to other olefin copolymers, P(B1-*ran*-E) shows a strong melt memory effect, even beyond the equilibrium melting

temperature. The three temperature domains were determined, and it was found that the polymorphism of the final material is strongly dependent on the T_s value. In addition, *Domain III* could be divided into two temperature regions. Additionally, the effect of self-nuclei on nucleation density and spherulitic growth rate was also measured.

2. Experimental section

2.1 Materials.

The butene-1/ethylene statistic copolymer P(B1-*ran*-E), trade name PB8340M, was purchased from Lyondell Basell Industries. The physical properties are listed in Table 1.

Table 1. Characterization of P(B1-*ran*-E) sample

	Trade name	Melt flow rate (MFR) (190 ºC/2.16 kg)	M_w (kg/mol)	PDI	Content of comonomer (Characterized by NMR)[41]	$T_{m, 1}$ (ºC, form I)	$T_{m,2}$ (ºC, form II)
P(B1-*ran*-E)	PB8340M	4	28.1	4.25	4.8%	113	97

2.2 Differential scanning calorimetry (DSC).

The self-nucleation behavior of P(B1-*ran*-E) was investigated employing a TA differential scanning calorimeter (Q2000). The instrument was calibrated with indium and measurements were carried out under nitrogen atmosphere (50 ml/min). P(B1-*ran*-E) samples weighing about 5~6 mg in sealed aluminum pans were employed. Based on the standard self-nucleation procedure proposed by Lotz et al., [7,11] the thermal treatment could be divided into two parts: sample preparation and self-nucleation stage

(as shown in Figure 1).

(a) Sample preparation stage: all samples were heated to 200 ℃ for 5 min erasing their thermal history. Following that, they were cooled to 0 ℃ at a rate of 10 ℃ /min, and then held at this temperature for 3 min. During this short low temperature thermal treatment, a small amount of form II crystals can transform into the more stable form I. Therefore, P(B1-*ran*-E) samples with mixed polymorphic crystal forms were generated.

(b) Self-nucleation stage: the polymorphic P(B1-*ran*-E) samples were heated to different SN temperatures, T_s, for 5 min. Then all samples were cooled to 0 ℃ (and held there for 3 min) and then heated to 200 ℃ to check the SN behavior of the material.
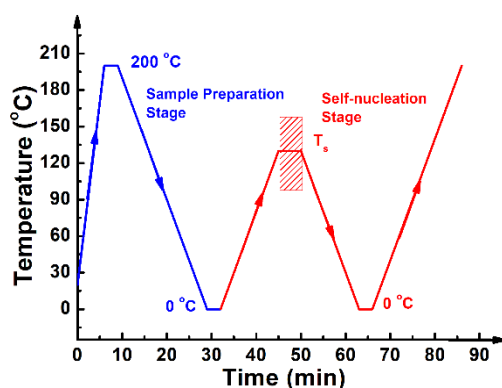

Figure 1. Standard self-nucleation protocols for PB1-*ran*-PE.

2.3 Polarized optical microscopy observation (PLOM).

The morphology of the P(B1-*ran*-E) sample after cooling from the isotropic or the self-nucleated melt was observed *in situ* by an Olympus BX51 polarized optical microscope equipped with a Canon 40D camera. A calibrated Linkam 600 hot stage was used to perform the thermal treatment. Before the observation, the PB1-*ran*-PE samples were hot pressed into films with a thickness of ca. 70 μm and sandwiched in

7

between of two glass slides.

3. Results and discussion

3.1 Self-nucleation behavior of P(B1-*ran*-E).

DSC cooling and heating curves after annealing at T_s are summarized in Figures 2a and 2b, and the detailed classification of the three SN domains obtained is illustrated in Figure 3.

(1) Domain I (Isotropic melt Domain, T_s values above 155 ^{o}C).

When the T_s temperature is higher than 155 ^{o}C (red curves in Figures 2a and 2b), only one monomodal crystallization peak shows up at relatively low temperatures (38 ^{o}C) during the cooling process (Figure 2a). In this situation, all crystals are molten because of the high temperature treatment. According to the definition by Lotz et al., [11] this T_s temperature range (above 155 ^{o}C) can be classified as *Domain I* (red line shown in Figure 3a). Besides that, double melting peaks are observed during subsequent heating scans (Figure 2b). The very small endothermic peak at 117 ^{o}C (signaled with black arrows in Figure 2b) is due to the melting of a small population of form I crystals, which formed previously via phase transition from the kinetically favored form II promoted by the 3 min thermal treatment at 0 ^{o}C. [42-45]

(2) Domain II (Self-nucleation domain, T_s values are in between 124 and 155 ^{o}C).

As the T_s value is reduced (see blue curves in Figure 2a), the crystallization temperature of P(B1-*ran*-E) starts to increase, indicating that the sample is being self-nucleated.
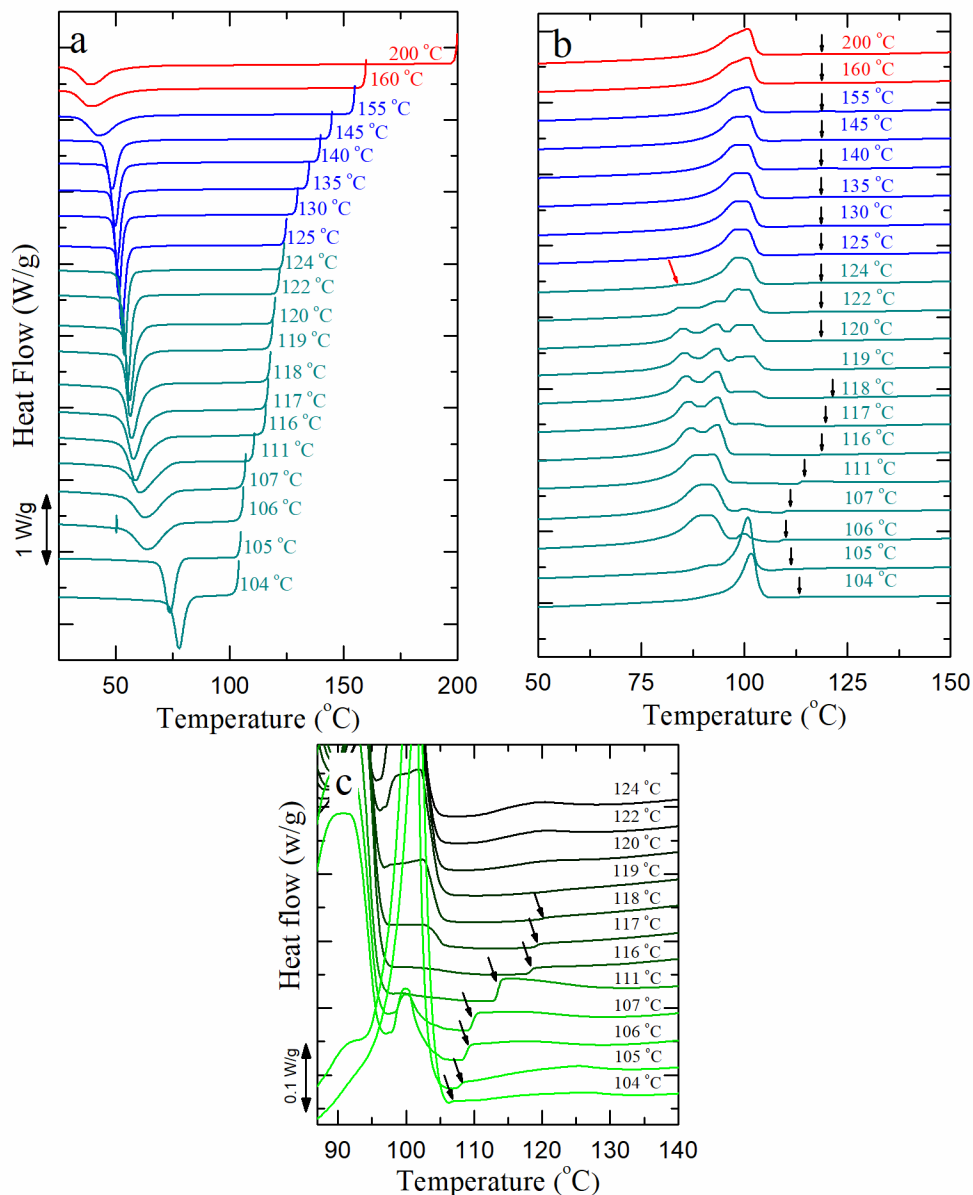
Figure 2. Self-nucleation behavior of P(B1-*ran*-E). (a) DSC cooling scans from different T_s temperatures; (b) subsequent heating process; (c) close view of selected heating curves in *Domain III*. Black arrows indicate the peak value for the melting of form I crystals.

Two melting peaks are observed during the heating runs in Figure 2b, when the T_s value is above 124 °C. [38] In other words, the self-nucleation effect generated in this T_s

temperature domain does not change the polymorphism of P(B1-*ran*-E), remaining similar to that described in *Domain I*.
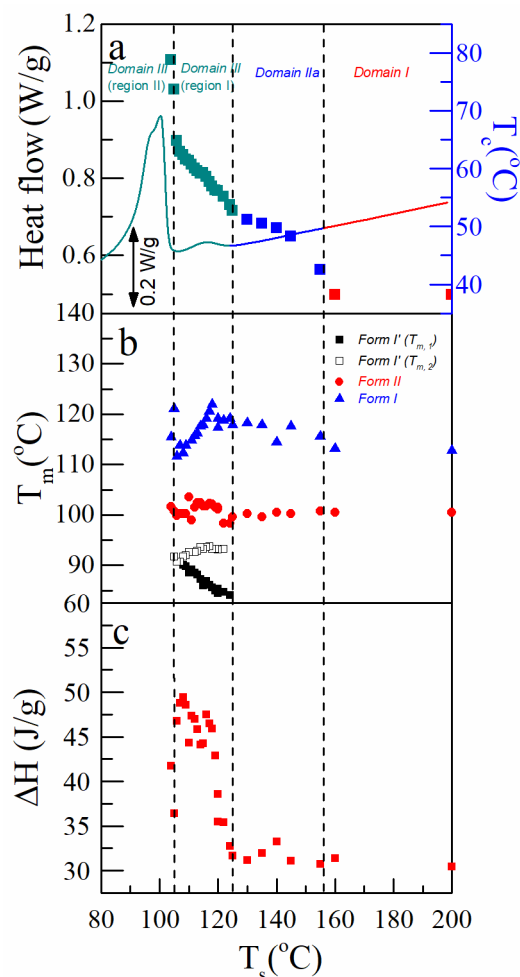

Figure 3. (a) Summary of the self-nucleation domains on top of a standard DSC heating trace for P(B1-*ran*-E), where the data points represent the crystallization temperatures as a function of T_s values; (b) Melting temperatures for all crystal forms and total melting enthalpy; (c) Enthalpy values as a function of the T_s temperature.

Comparing with the homopolymer PB-1, which possesses a narrow *Domain II*, it is noticeable that self-nuclei of P(B1-ran-E) can survive even above the equilibrium

melting temperature of PB-1 homopolymer (148 $^\circ$C) [46], alike other polyethylene copolymers. [15,16,29] In particular, based on the definition proposed by Müller et al, [7,17,26] *Domain II* could be divided into *Domain IIa,* if the heat flow signal reaches the baseline (indicating all crystals have melted), and *Domain IIb*, if the signal is still within the melting endotherm (indicating that a small crystal population or crystal fragments remain that can act as self-seeds). For P(B1-*ran*-E), obviously the calorimetric signal is well in the baseline region in the entire *Domain II*. Thus, only *Domain IIa* (melt memory sub-domain) exists for this material.

(3) Domain III (Self-nucleation and annealing domain, T_s values below 124 $^\circ$C).

P(B1-*ran*-E) crystals in this T_s domain could only partially melt (see green curves in Figures 2a and 2b). In this situation, the remaining crystals (form II or form I) could serve as the best nucleating agents, whereas different polymorphs could be generated. Apart from the normal form II and transformed form I, additional double melting peaks are observed at relatively low temperatures (83 to 93 $^\circ$C), referring to the melting of the original structure and final melting of form I' (see Figure 2b). Based on the detailed analysis of the self-nucleation behavior of PB-1 homopolymer, Cavallo et al. [33] found that form I' crystals could only be induced in the presence of form I crystals.

In principle, the division between *Domain II* and *III* is distinguished by the appearance of an annealing peak of the unmolten crystals in the final heating run. [7,17] In our case, the form I annealing peak is too small to be detected due to its low amount. Therefore, we need to differentiate *Domain III* from *Domain II* by recognizing the formation of form I' from the remaining form I crystals. A close-up view of the final

heating curves in *Domain III* is shown in Figure 2c. Clearly, additional low temperature melting peaks of form I' show up when T_s is reduced below 124 $^{\circ}$C, indicating that the self-nucleation temperature enters into *Domain III*.

In particular, when the T_s value is even below 105 $^{\circ}$C, a large quantity of form II crystals could be obtained again at the expense of form I' crystals. Here, also some residual form II crystals could survive and be annealed, thus serving as the most efficient self-seeds for form II. As the growth rate of form II is much faster than that of form I', the crystallization of trigonal crystals, form I', could be strongly suppressed. In this special case, *Domain III* can be divided into two regions: (1) *Region I* (105-124 $^{\circ}$C), where form I crystals and the melt memory of form II remain in the sample, as both *Domain III* and *Domain IIa* for form I and form II, respectively, coexist; (2) *Region II* (below 105 $^{\circ}$C), where form I and form II crystals survive in the material, representing *Domain III* for both form II and form I.

The peculiar melting behavior of form I crystals in *Domain III* is summarized in Figure 2c in close view. When the T_s value is above 119 $^{\circ}$C, nearly all form I crystals previously formed at 0 $^{\circ}$C are molten. A large amount of form II can still be obtained during the following cooling process from T_s, triggered by the self-nucleating melt memory effect. After that, the crystallized form II crystals partially transformed into stable form I crystals during the second 0 $^{\circ}$C thermal conditioning procedure. Thus, a symmetric small melting peak at 118 $^{\circ}$C appears in the final heating run.

However, when the T_s value is below 119 $^{\circ}$C, an asymmetric peak of form I crystals at a certain temperature shows up. In this situation, mainly form I' could be nucleated

because of the large amount of remaining form I crystals. Therefore, nearly no form I crystals could be transformed during the second 0 °C thermal conditioning process, and the melting temperature of these form I crystals decreases with the reduction of T_s value because of the expected annealing process. Hence, form I crystals in the final heating stage are basically obtained from two contributions: (1) transformed form I crystals during the first low temperature thermal conditioning, which still survive at the T_s temperature applied; (2) transformed form I crystals during the second thermal conditioning at low temperature determined by the amount of form II crystals crystallized during the second cooling process.

The melting temperature for the different P(B1-*ran*-E) crystal forms and total melting enthalpy as a function of T_s value are summarized in Figures 3b and 3c. The melting temperatures of form II and the corresponding transformed form I crystals practically stay constant (Figure 3b). However, in *region I* of *Domain III*, due to partial melting and annealing effect, the melting temperature of form I crystals decreases with the decrease of T_s values (see Figure 3b). As to the self-nucleated form I′, the melting peak of the original structure, $T_{m,1}$, increases with the increase of crystallization temperature satisfying the Hoffman-Weeks relationship. [47] But the final melting point, $T_{m,2}$ almost does not change with T_s.

Based on intra-crystalline chain dynamic (ICD) detected by NMR spectroscopy, semi-crystalline polymers can be divided into two classes: crystal-fixed and crystal-mobile polymers. [48] Recently, a detailed small angle X-ray scattering analysis on PB-1 was published by Men et al. [45] Based on their description, form I and form II can be

classified into crystal-fixed and crystal-mobile polymorphs, respectively.

Since form I and form I' share similar trigonal crystal structure and chain conformation, it is reasonable to assume form I' also has an extremely slow ICD behavior (i.e., crystal-fixed). According to observations from Thurn-Albrecht et al., [39,49] chain dynamics in a crystal-fixed polymer are quite slow and almost no thickening happens during isothermal crystallization process. It is very likely that the lamellar thickness of form I' is close to the critical lamellar thickness d_c^*, and the melting temperature of the original structure approaches T_c at zero heating rate. Thus, $T_{m,1}$ for form I' is strongly influenced by T_c which corresponds to the similar melting behavior of poly(ε-caprolactone).

On the other hand, for crystal-mobile polymers like polyethylene oxide and form II of PB-1, the lamellar thickness increases much faster than crystal growth rate and thus thickening could be accomplished even before primary crystallization. In our case, it is reasonable to assume that the lamellar thickness of form II is much thicker than d_c^*. Thus, the melting temperature of form II is nearly constant for all T_s values.

The total melting enthalpy (ΔH) of P(B1-ran-E) strongly depends on the polymorphic composition because of the higher melting enthalpy values estimated for 100 % crystallinity in trigonal crystals (141 J/g) with respect to the value estimated for form II (62 J/g). [46] Only form II and a small amount of transformed form I crystals could be generated in *Domain I and II*, so ΔH in these two domains is constant and relatively low (see Figure 3c). However, the melting enthalpy increases with further reductions in T_s values due to the generation of form I' in *region I* of *Domain III*, and

drops back to relatively low value in *region II* (Figure 3c).

Based on the above analysis, it is clear that the T_s value can strongly influence the nucleation behavior of P(B1-*ran*-E). Different polymorphs can be generated when the material is cooled from different self-nucleation temperature domains. The remaining crystalline form I self-seeds in *Domain III* could nucleate the formation of form I' crystals with similar structure. On the other hand, melt memory in *Domain II* could only act as self-nuclei for the kinetically favored form II.

2.2 The consequences of the memory: nucleation density or growth rate.

Usually, it is considered that self-nuclei can act as highly efficient nucleating agents, which increase the nucleation density in the subsequent crystallization process. However, according to the description by Strobl et al.,[20] the authors consider melt memory as a kind of mesophase, which can be filled-in with the crystals when the sample is cooled to low temperatures. Therefore, both nucleation density and spherulite growth rate should be promoted.
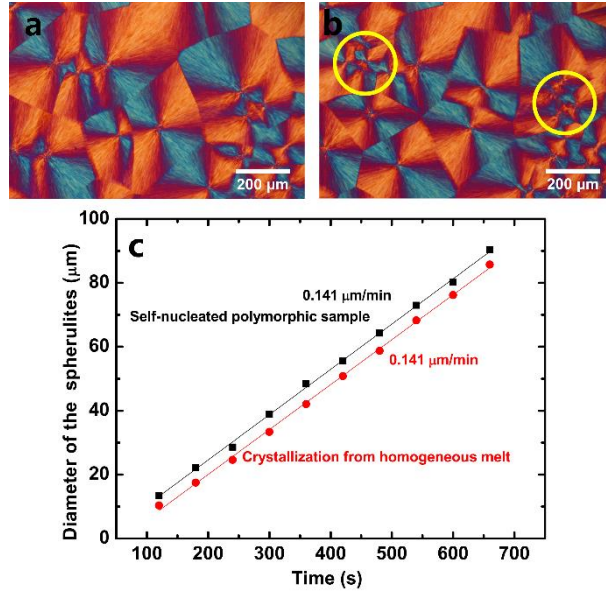
Figure 4. In situ PLOM observation of the P(B1-*ran*-E) crystallized with different thermal histories. The samples were first crystallized isothermally at 75 °C (a), then cooled to 0 °C for 3 min to produce some form I crystals. Following that, the sample was heated to 148 °C for 5 min and crystalized 75 °C again (b). (c) Measured diameters of the P(B1-*ran*-E) spherulites vs crystallization time during the former two isothermal crystallization processes.

Figure 4 shows the *in situ* PLOM observations of P(B1-*ran*-E) samples crystallizing at 75 °C after cooling from the isotropic or the self-nucleated melt. Figure 4a displays the morphology of P(B1-*ran*-E) after crystallization at 75 °C. Then the sample is cooled to 0 °C for 3 min and heated to a T_s temperature of 148 °C for 5 min to produce some active nuclei. Following that, the sample was quenched to 75 °C again for the second isothermal crystallization process as shown in Figure 4b. Comparing the two different morphologies, it was found that several additional spherulites are generated in the second crystallization procedure, highlighted in the

16

yellow circles. It confirms that nucleation density can be enhanced by the melt memory effect.

We also measured the size of the spherulites at different times and calculated the spherulitic growth rates (Figure 4c). The two straight lines representing the relationship between spherulite diameter and time are parallel, indicating that the lamellar growth rate does not change with the presence of non-crystalline self-nuclei. Thus, this observation proves that melt memory can only promote an increase in nucleation density but does not cause any change in spherulitic growth rate.

The PLOM results are in line with the notion that self-seeds (*Domain IIb*) or self-nuclei coming from melt memory effects (*Domain IIa*) cause an enhancement in primary nucleation density, without altering crystal growth.

4. Conclusions

In this study, the self-nucleation behavior of a typical statistical copolymer, P(B1-*ran*-E) is investigated. Like other polyolefin copolymers, P(B1-*ran*-E) displays a strong melt memory effect within a wide temperature range. Due to the complicated solid-solid transitions in this material, different polymorphic forms can be obtained by cooling from different T_s temperatures. Three temperatures domains are distinguished and a clear transition appears in between *Domain II* and *Domain III,* indicating that the presence of unmolten form I crystals could lead to the formation of form I' by self-seeding. Based on this observation, *Domain III* could be divided into two temperature regions. In addition, PLOM observation confirms that nucleation density increases if

the sample is cooled from self-nucleated melts, as expected, but on the other hand do not affect spherulitic growth rates.

AUTHOR INFORMATION

Corresponding Authors

*E-mails: dario.cavallo@unige.it and alejandrojesus.muller@ehu.es

Notes

The authors declare no competing financial interest.

References

[1]. Rabesiaka, J.; Kovacs, A. J. Journal of Applied Physics 1961, 32, 2314-2320.

[2]. Bastiaansen, C. W. M.; Meyer, H. E. H.; Lemstra, P. J. Polymer Bulletin 1990, 31, 1435-1440.

[3]. Alfonso, G. C.; Ziabicki, A. Colloid and Polymer Science 1995, 273, 317-323.

[4]. Alfonso, G. C.; Scardigli, P. Macromol. Symp. 1997, 118, 323-328.

[5]. Maus, A.; Hempel, E.; Thurn-Albrecht, T.; Saalwachter, K. Eur Phys J E Soft Matter 2007, 23, 91-101.

[6]. Gao, H.; Vadlamudi, M.; Alamo, R. G.; Hu, W. Macromolecules 2013, 46, 6498-6506.

[7]. Michell, R. M.; Mugica, A.; Zubitur, M.; Müller, A. J. In Polymer Crystallization I: From Chain Microstructure to Processing; Auriemma, F.; Alfonso, G. C.; DeRosa, C., Eds.; Springer: Gewerbestrasse, 2017, p 215.

[8]. Blundell, D. J.; Keller, A.; Kovacs, A. J. Polym. Lett. 1966, 4, 481-486.

[9]. J., B. D.; Keller, A. Journal of Macromolecular Science 1968, 2, 301-336.

[10].   Vidotto, G.; Lévy, D.; Kovacs, A. J. Kolloid-Zeitschrift & Zeitschrift für Polymere 1969, 230, 289-305.

[11].   Fillon, B.; Thierry, A.; Wittmann, J. C.; Lotz, B. Journal of Polymer Science Part B-Polymer Physics 1993, 31, 1407-1424.

[12].   Sabino, M. A.; Ronca, G.; Müller, A. J. J. Mater. Sci. 2000, 35, 5071-5084.

[13].   Schneider, S.; Drujon, X.; Lotz, B.; Wittman, J. C. Polymer 2001, 42, 8787-8798.

[14].   Müller, A. J.; Michell, R. M.; Pérez, R. A.; Lorenzo, A. T. European Polymer Journal 2015, 65, 132-154.

[15].   Reid, B. O.; Vadlamudi, M.; Mamun, A.; Janani, H.; Gao, H.; Hu, W.; Alamo, R. G. Macromolecules 2013, 46, 6485-6497.

[16].   Chen, X.; Wignall, G. D.; He, L.; Lopez-Barron, C.; Alamo, R. G. Macromolecules 2017, 50, 4406-4414.

[17].   Sangroniz, L.; Cavallo, D.; Müller, A. J. Macromolecules 2020, 53, 4581-4604.

[18].   Strobl, G. Eur. Phys. J. E 2000, 3, 165-183.

[19].   Häfele, A.; Heck, B.; Hippler, T.; Kawai, T.; Kohn, P.; Strobl, G. Eur. Phys. J. E 2005, 16, 217-224.

[20].   Häfele, A.; Heck., B.; Kawai, T.; Kohn, P.; Strobl, G. Eur. Phys. J. E 2005, 16.

[21].   Luo, C.; Sommer, J.-U. Acs Macro Lett. 2013, 2, 31-34.

[22].   Luo, C.; Sommer, J.-U. Phys. Rev. Lett. 2014, 112, 195702.

[23].   C, L.; Sommer, J.-U. Macromolecules 2016, 49, 9017-9025.

[24].   Luo, C.; Sommer, J.-U. Acs Macro Lett. 2016, 5, 30-34.

[25].   Lorenzo, A. T.; Arnal, M. L.; Sanchez, J. J.; Müller, A. J. Journal of Polymer Science Part B-Polymer Physics 2006, 44, 1738-1750.

[26].   Liu, X. R.; Wang, Y.; Wang, Z. F.; Cavallo, D.; Müller, A. J.; Zhu, P.; Zhao, Y.; Dong, X.; Wang, D. J. Polymer 2020, 188.

[27].   Sangroniz, L.; Sangroniz, A.; Meabe, L.; Basterretxea, A.; Sardon, H.; Cavallo, D.; Müller, A. J. Macromolecules 2020, 53, 4874-4881.

[28].   Sangroniz, L.; Ocando, C.; Cavallo, D.; Müller, A. Polymers 2020, 12, 2796.

[29].   Marxsen, S. F.; Alamo, R. G. Polymer 2019, 168, 168-177.

[30].   Somani, R. H.; Yang, L.; Hsiao, B. S. Physica A 2002, 304, 145-157.

[31].   Somani, R. H.; Sics, I.; Hsiao, B. S. J. Polym. Sci, Part B: Polym. Phys. 2006, 44, 3553-3570.

[32].   Geng, Y.; Wang, G.; Cong, Y.; Bai, L.; Li, L.; Yang, C. Macromolecules 2009, 42, 4751-4757.

[33].   Cavallo, D.; Gardella, L.; Portale, G.; Müller, A. J.; Alfonso, G. C. Polymer 2014, 55, 137-142.

[34].   Cui, K. P.; Liu, D.; Ji, Y. X.; Huang, N. D.; Ma, Z.; Wang, Z.; Lv, F.; Yang, H. R.; Li, L. B. Macromolecules 2015, 48, 694-699.

[35].   Cavallo, D.; Gardella, L.; Portale, G.; Müller, A. J.; Alfonso, G. C. Polymer 2013, 54, 4637-4644.

[36].   Su, F. M.; Li, X. Y.; Zhou, W. M.; Zhu, S. S.; Ji, Y. X.; Wang, Z.; Qi, Z. M.; Li, L. B. Macromolecules 2013, 46, 7399-7405.

[37].   Cavallo, D.; Gardella, L.; Portale, G.; Müller, A. J.; Alfonso, G. C. Macromolecules 2014, 47, 870-873.

[38].   Cavallo, D.; Zhang, L.; Sics, I.; Alfonso, G. C.; Dumas, P.; Marco, C.; Ellis, G. Cryst. Eng. Comm 2016, 18, 816-828.

[39].   Schulz, M.; Seidlitz, A.; Petzold, A.; Thurn-Albrecht, T. Polymer 2020, 196, 122441.

[40].   Wang, Z.; Dong, X.; Cavallo, D.; Müller, A. J.; Wang, D. Macromolecules 2018, 51, 6034-6046.

[41].   Hsieh, E. T.; Randall, J. C. Macromolecules 1982, 15, 353-360.

[42].   Qiao, Y. N.; Wang, Q.; Men, Y. F. Macromolecules 2016, 49, 5126-5136.

[43].   Qiao, Y.; Men, Y. Macromolecules 2017, 50, 5490-5497.

[44].   Qiao, Y.; Yang, F.; Lu, Y.; Liu, P.; Li, Y.; Men, Y. Macromolecules 2018, 51, 8298-8305.

[45].   Qiao, Y.; Schulz, M.; Wang, H.; Chen, R.; Schäfer, M.; Thurn-Albrecht, T.; Men, Y. Polymer 2020, 195, 122425.

[46].   Pyda, M.; Wunderlich, B. Macromolecules 1999, 32, 2044-2050.

[47].   Hoffman, J. D.; Lauritzen, J. I. Journal of Research of the National Bureau of Standards 1961, A 65, 297-336.

[48].   Hu, W. G.; Schmidt-Rohr, K. Acta Polymerica 1999, 50, 271-285.

[49].   Schulz, M.; Seidlitz, A.; Kurz, R.; Bärenwald, R.; Petzold, A.; Saalwächter, K.; Thurn-Albrecht, T. Macromolecules 2018, 51, 8377-8385.

Table of content

The complex self-nucleation behavior of a polybutene-1 random copolymer, P(B1-*ran*-E), that exhibits polymorphic behavior, is studied in detail. Trigonal form I' could be obtained when form I crystals were present (*Domain III*), while melt memory induced self-nuclei (*Domain IIa*) could only promote the nucleation of kinetically favored form II. Optical microscopy results indicate that melt memory can only enhance nucleation density but it cannot affect spherulitic growth rate.

Zefan Wang[1,2], Xia Dong[1,2], Dario Cavallo*, Dujin Wang and Alejandro J. Müller*

Peculiar self-nucleation behavior of a polybutene-1 copolymer